LLNL-JRNL-405016

LAWRENCE LIVERMORE NATIONAL LABORATORY

One-Dimensional Neutron Imager for the Sandia Z Facility

D. N. Fittinghoff, D. E. Bower, J. R. Hollaway, B. A. Jacoby, P. B. Weiss, R. Buckles, T. Sammons, L. A. McPherson, C. Ruiz, G. Chandler, J. Torres, R. Leeper, G. Cooper, A. Nelson

June 30, 2008

Review of Scientific Instruments

One-Dimensional Neutron Imager for the Sandia Z Facility[1]

David N. Fittinghoff, Dan E. Bower, James R. Hollaway, Barry A. Jacoby and Paul B. Weiss

Lawrence Livermore National Laboratory, Livermore CA 94550, fittinghoff1@llnl.gov

Robert A. Buckles and Timothy J. Sammons

National Security Technologies, LLC, Livermore, CA 94550

Leroy A. McPherson Jr., Carlos L. Ruiz, Gordon A. Chandler, José A. Torres, and Ramon J. Leeper

Sandia National Laboratory, Albuquerque, NM 87185-1193

Gary W. Cooper and Alan J. Nelson

University of New Mexico, Albuquerque, NM, 87131

A multi-institution collaboration is developing a neutron imaging system for the Sandia Z Facility. The initial system design is for slit-aperture imaging system capable of obtaining a 1-D image of a 2.45-MeV source producing 5×10^{12} neutrons with a resolution of 320 µm along the axial dimension of the plasma, but the design being developed can be modified for 2-D imaging and imaging of DT neutrons with other resolutions. This

---

[1] Contributed paper, published as part of the Proceedings of the 17th Topical Conference on High-Temperature Plasma Diagnostics, New Mexico, May 2008

system will allow us to understand the spatial production of neutrons in the plasmas produced at the Z Facility.

PACS: 52.70Nc, 52.58.Lq, 03.75.Be

Introduction and Design

The Sandia Z Pinch is designed to allow the study of the high-energy density physics and inertial confinement fusion[1-3]. Experiments using the Z-pinch are capable of producing neutrons from deuterium or deuterium and tritium targets. While a variety of diagnostics have been fielded at the facility, to date no system has been successfully fielded for imaging the production of the neutrons. We are developing a one-dimensional neutron imaging system for use on the upgraded Z machine.

While the exact source distribution is not known, since the system is expected to have strong radial symmetry, we are imaging only in one-dimension along the axis to improve the S/N. We are designing to be able to image a source of 2.45-MeV neutrons that produces 5×10^{12} neutrons into 4π. The target axial resolution will be ~320 μm with a field of view of 7 mm. The minimum source size could be below the resolution limit while the maximum design source size is 0.5-mm in diameter by 5-mm long in the axial dimension (2.5 mm^2). We discuss the resolution in detail and the expected signal to noise in the section on expected image quality below. Other requirements are that the system can be extended to two-dimensional imaging in the future, that it be able to survive the shock and electromagnetic environment that exists at the Z-facility and that it can be aligned rapidly prior to the shot, which is critical since the source is known to move by about a millimeter during the pump down of the vacuum system at Z.

Design

The system that we have designed is an aperture imaging system similar to pinhole imaging system or penumbral imaging systems for neutrons[4-10], which use thick, high-density apertures to define a neutron image at an image plane. The image is detected with a scintillating material viewed by a camera. In our system, we take advantage of the expected symmetry and use a slit aperture as shown in Fig. 1. For sources that are small across the dimension of the slit, the slit aperture does not significantly increase the amplitude of the signal relative to the amplitude of the signal from a pinhole aperture of the same resolution. Using a slit does, however, allow integration of the image along the dimension of the slit to collapse the image to one-dimension and increase the signal to noise, which is useful for potentially weak sources. The aperture mounting system is designed to allow replacement of the slit aperture with other apertures and is thus suitable for 2-D imaging as well as 1-D imaging.

In our design, the 90% tungsten heavy metal, slit aperture is placed 53.7 cm from the source, and a 75-mm diameter, 50-mm thick, BCF-99-55 scintillating fiber bundle with 250-µm square fibers is placed at 300 cm from the source for a magnification of 4.58. The BCF-99-55 (made by Saint Gobain) is a binary scintillator using higher doping of the same wavelength shifter that is used in BCF-12 but without the UV fluorescing material that is present in that tertiary scintillator. This eliminates the conversion stage from UV to visible wavelengths, which suffers high losses in fibers smaller than the ~300-µm mean free path of the UV in the fiber material. BCF-99-55 has a peak emission wavelength of ~435 nm, a decay time of 3.2 ns, a carbon density of ~4.8×10^{22} atoms/cc and a hydrogen density of ~4.8×10^{22} atoms/cc. It produces ~8000 photons/MeV for a minimum ionizing particle.

The slit separation along the axial dimension is 204 μm with a 1.8-cm long straight section, and 13.45-mradians tapered front and back tapered sections. In the radial dimension, the full angle of the slit opening is 15 mradians and is designed to give a radial field of view of 0.5 cm at the source to accommodate any side-to-side motion of the source. The overall length of the body of the slit aperture is 15 inches, a length which is longer than necessary for 2.45 MeV neutrons, but which provide low (~10^{-5}) background for any future work at 14.1 MeV. The image produced in the scintillator will be obtained using a Princeton Instruments PIMAX 1300 CCD camera that is fiber coupled to the scintillator via a 3-to-1 fiber taper and a 26-mm wound fiber bundle ~3-m long. The CCD camera has a 25-mm diameter gated intensifier (HBf filmless) with a minimum gate speed that is <7 ns.

Expected Image Quality

The on-axis point spread function of the slit aperture optical system has a full-width at half maximum of 248-μm when projected back to the source. We have numerically convolved a ray-tracing calculation of this on-axis point spread function at the scintillator with the expected deposition in the scintillator (~400-μm full-width at half maximum), with the scintillator fiber size and with the 80-μm size of the 4x4 binned CCD pixels projected to the scintillator. Using the assumption that this convolved point spread function may be used off-axis, we find that the expected resolution according to the Houston Criterion, for which sources are resolved when separated by the full-width at half maximum of the line [11], is 320-μm. Using the Sparrow Criterion, for which two sources are resolved when the second derivative of the combined point spread function for the two sources is zero[12], the expected resolution is 264 μm. Lineouts along the resolution dimension of the expected 1-D image for two point sources separated by this resolution are shown in Fig. 2. The axial field of view is estimated to have a full width of 1.2 cm, which is larger than our requirement, but we do expect some roll off of the signal due to shading over that region that is unavoidable with to the resolution requirement. A flat field simulation indicates that the signal will fall off by a factor of 3.75 from the center of the field to the edge.

The real limit to the quality of the images will be the signal-to-noise. Without considering any background, the best-case limit to the signal-to noise is the statistical or "shot" noise in the detection of the neutrons at the scintillator. To investigate this, we have performed a direct calculation of the expected number of neutrons interacting in each fiber based on the expected yield of the source, the area of the source, the transmission of the metal filters (shields required to protect equipment in the Z environment), the solid angle of the source viewed by a detector element through the aperture, and the fraction of incident neutrons that interact in the scintillator. Since each fiber in the scintillator combines the light produced from the neutrons that interact in it, we chose to calculate the neutron statistics in each fiber in the image assuming a uniform amplitude source. For our current design, the source yield is $5x10^{12}$ neutrons in 4π. The filter transmission is 0.65 (approximately 1.5 inches of iron) and the fraction of the incident neutrons that interact in the scintillator is ~0.4. Thus, for a sub-resolution source (less than 320 μm in diameter), approximately 558 neutrons will interact in each 250-μm by 250-µm fiber, and the expected signal-to-noise ratio (SNR) based on neutron statistics will be 23.6. Summing the signals from the 172 fibers across the unresolved dimension of the image, would improve the SNR to 310 in the absence of other noise sources. For constant neutron yield, the SNR will decrease as the source becomes larger, and for the maximum expected possible source size of 0.5 cm by 0.5 mm, the SNR based on neutron statistics will be 6 for a single fiber and 78.5 for the signal summed over the unresolved dimension of the image.

Alignment

One of the most significant challenges of fielding a neutron imaging system at Z is that the aperture must be close to the source to allow enough neutrons to pass through the aperture for measurement, which means that the aperture must be placed inside the vacuum chamber. Since the Z source is destroyed and rebuilt after each shot and since the source moves during pump down, this means that the pinhole must be realigned on every shot after the chamber has been pumped down. Given the relatively tight alignment tolerances of the slit, which are an angular pitch tolerance of ±6.5 mradians, a position tolerance of ±0.35 cm and a roll tolerance of ±21.7 mradians, fine adjustments must be made using motors in vacuum with a reference system that can be operated from outside the chamber.

Our current plan is to have a mirror with cross hairs mounted to the end of the pinhole furthest from the source. The mirror will be aligned to the slit on the bench top and fixed in place before the pinhole is placed inside the chamber. On each shot, the pinhole will be translated off the line of sight to allow a telescope with a collinear laser beam to sight the source. The pinhole will then be translated into the line of sight. The telescope will be used to center the cross hairs on the line of sight and adjust the roll of the pinhole. The laser will then be retroreflected from the mirror to set the pich and yaw angles. The same method will be used to align the scintillator, and this method should be sufficiently accurate for use in 2-D imaging as well as for the initial 1-D imaging.

Z Environment

In addition to the neutrons that we want to image, the Z-machine creates a strong x-ray and γ-ray photon pulse, an electromagnetic pulse, debris from the destruction of the source and a shock that propagates from the machine throughout the building. These effects require mitigation and complicate the design of the system.

The debris inside the chamber ranges from fine metallic dust to bullet-like chunks of metal, and the Z-machine has a cylindrical blast shield to prevent the larger particles from destroying equipment. For our system, the main blast shield will be open to allow alignment, and custom shields to protect the pinhole assembly and the vacuum window on our line of sight will be required. Additionally, we will use local dust shields over the motors and stages that are used for alignment to prevent buildup of metallic dust on electronics or drive shafts that could affect their operation.

The x-ray and γ-ray photon pulse can affect the system by exciting the scintillator and the optical taper and fiber bundle directly as well as by creating background starring in the CCD. While the blast shield does attenuate the x-rays and γ-rays relative to its' attenuation of the neutrons, the hard x-rays and γ-rays are still significant and expected to produce signal in the scintillator that will arrive at the speed of light. Since even the 14-MeV neutrons that would be produced by a deuterium-tritium reaction travel well below the speed of light, they would arrive 48-ns after the hard x-rays and γ-rays, which allows them to be gated out. For 2.45 MeV neutrons, the temporal separation between the γ-ray signal and the neutrons is 129 ns, and for 14.1 MeV neutrons it is 49 ns. The <7-ns gate speed of the intensifier will allow us to gate to eliminate the γ-ray signal from the source. While some residual γ-ray signal is possible due to the 3.2-ns decay time of the scintillator, our previous measurements indicate that the γ-ray signal on the scintillator is near the same size as the neutron signal, and we expect the residual γ-ray signal to be insignificant.

To reduce the number of energetic photons and neutrons that can reach the detector system by going around the aperture, we will also use a 6” thick tungsten collimator directly behind the aperture to shadow the detection system. We also are designing to allow local shielding around the CCD camera if it is required to reduce back- or side-scattering from within the building.

One of the most difficult effects to design for is the physical shock wave created by the machine, which propagates both inside and outside the machine. We have measured 13-g shocks on the stack inside the machine. To compensate for these shocks, we are using both heavier and stronger parts and motors and shock dampening mounts such as the Barry T94-AB-110 on the aperture positioning and imaging assemblies, and by using a wound fiber bundle between the scintillator and taper and the CCD, we hope to reduce torque that could damage the intensifier in the CCD, which is already designed to be spring-loaded to reduce such damage. The fiber bundle is also long enough to allow the CCD camera to be placed where it can be more easily shielded or shock mounted. The magnification requirements for the system place the scintillator 300 cm from the source, which is immediately outside the vacuum spool inside the boats that create lines of sight through the water lines between the capacitor banks and magnetically insulated transmission lines. This location is low on space and difficult to access so separating the CCD from the scintillator and taper has the additional advantage of improving space usage and access to the CCD camera.

To mitigate the electromagnetic pulse produced by the Z-machine, we are using EMI shielding for all electronics, including running any metal cables through 90-dB conduits. We have also tested the drive motors for the positioners and shown that they can survive inside the Z vacuum chamber, but if necessary, they could be replaced on each shot.

Conclusions

In conclusion, our team is developing a neutron slit-aperture imaging system for use on the Sandia Z-pinch. This system will begin as a 1-D imaging system capable of high signal-to-noise measurements with ~320-μm resolution for neutron yields of $5x10^{12}$ for source sizes up to 0.5-cm by 0.5-mm, but it could be converted to use as a 2-D imager as the neutron flux is increased. Most of the system has been designed, and fabrication and construction of the system has begun. We expect to be ready for imaging in February 2009. Prepared by LLNL under Contract DE-AC52-07NA27344.

References

[1] M. K. Matzen, Physics Of Plasmas **4** (5), 1519 (1997).

[2] M. K. Matzen, M. A. Sweeney, R. G. Adams et al., Physics Of Plasmas **12** (5) (2005).

[3] D. D. Ryutov, M. S. Derzon, and M. K. Matzen, Reviews of Modern Physics **72** (1), 167 (2000).

[4] R. A. Lerche, D. Ress, R. J. Ellis et al., Laser And Particle Beams **9** (1), 99 (1991).

[5] L. Disdier, A. Rouyer, A. Fedotoff et al., Review of Scientific Instruments **74** (3), 1832 (2003).
[6] V. Y. Glebov, D. D. Meyerhofer, T. C. Sangster et al., Review Of Scientific Instruments **77** (10) (2006).
[7] G. L. Morgan, R. R. Berggren, P. A. Bradley et al., Review Of Scientific Instruments **72** (1), 865 (2001).
[8] C. R. Christensen, C. W. Barnes, G. L. Morgan et al., Review Of Scientific Instruments **74** (5), 2690 (2003).
[9] J. P. Garconnet, O. Delage, D. Schirmann et al., Laser And Particle Beams **12** (3), 563 (1994).
[10] G. P. Grim, C. W. Barnes, P. A. Bradley et al., Journal De Physique Iv **133**, 913 (2006).
[11] W. V. Houston, Astrophysical Journal **64** (2), 81 (1926).
[12] C. M. Sparrow, Astrophysical Journal **44** (2), 76 (1916).

Figure Captions

Figure 1 Schematic of the slit imager concept. The neutron source is located at the origin or working point, and the x-axis is the axis of symmetry of the source. The system is only resolving in the x-dimension. The aperture is located a distance 53.7 cm from the source in the z-dimension, and a scintillator at z = 300 cm converts the neutrons to light. The two views are a) the view in the x-z plane showing the narrow dimension of the slit, which is a 1.8-cm long straight section with a separation of 200 µm with 13.45 mradian tapers at each end, and b) the view in the y-z plane where the aperture has an open angle of 15 mradians, which is chosen to give an unobstructed 0.5-cm field of view in the y dimension at the working point.

Figure 2 a) A lineout along the x-dimension of the simulated neutron image at the scintillator, with distances given at the source, for two point sources separated by 320 µm, the expected resolution using the Houston Criterion. b) A lineout along the x-dimension of the simulated neutron image at the scintillator, with distances given

at the source, for two point sources separated by 264 μm, the expected resolution using the Houston Criterion.

Figures

Figure 1

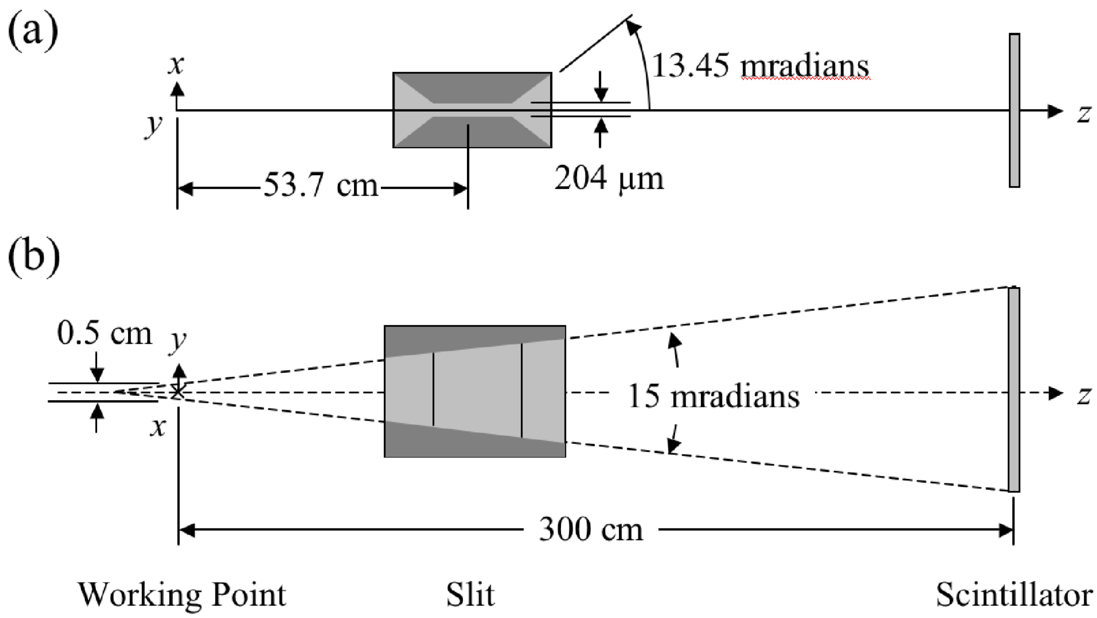

Figure 2

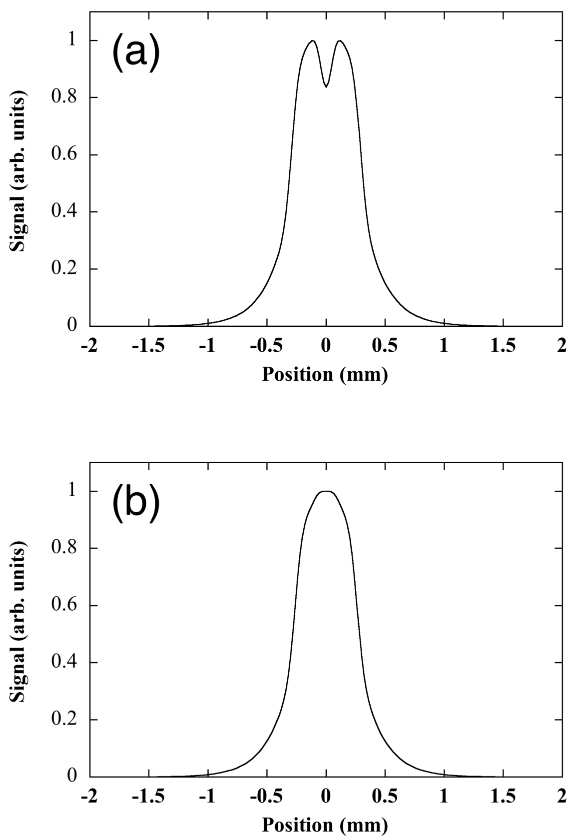
(a)
Signal (arb. units)
Position (mm)
0
0.2
0.4
0.6
0.8
1
-2
-1.5
-1
-0.5
0
0.5
1
1.5
2
(b)
Signal (arb. units)
Position (mm)